materials proceedings

MDPI

Proceeding Paper

Carbon-Based Perovskite Solar Cell †

Luigi Vesce [1,*], Maurizio Stefanelli [2] and Aldo Di Carlo [1,2]

[1] CHOSE, Centre for Hybrid and Organic Solar Energy, Department of Electronic Engineering, University of Rome "Tor Vergata", Via del Politecnico 1, 00133 Roma, Italy; aldo.dicarlo@uniroma2.it
[2] ISM-CNR, Istituto di Struttura della Materia, Consiglio Nazionale delle Ricerche, Via del Fosso del Cavaliere 100, 00133 Roma, Italy; maurizio.stefanelli@uniroma2.it
* Correspondence: vesce@ing.uniroma2.it
† Presented at the 4th International Online Conference on Nanomaterials, 5–19 May 2023; Available online: https://iocn2023.sciforum.net.

Abstract: In a short period, Perovskite solar cell (PSC) technology gained high efficiency and the broad attention because of key enabling physical and morphological features. One of the main obstacles to the PSC industrialization and commercialization deals with the demonstration of stable devices by adopting low-cost and reliable materials and fabrication methods. In the n-i-p structure the organic hole transporting layer and the metal counter-electrodes are the main causes of instability and high cost. Here, we substituted these two elements with a low-temperature and low-cost carbon-based counter electrode.

Keywords: perovskite solar cell; carbon; nanomaterial; low cost; hole transporting layer; stability; printing technique

Citation: Vesce, L.; Stefanelli, M.; Di Carlo, A. Carbon-Based Perovskite Solar Cell. *Mater. Proc.* **2023**, *5*, x. https://doi.org/10.3390/xxxxx
Published: 5 May 2023

1. Introduction

The constant and unceasing progress of the technology in different areas requires renewable and green energy sources [1]. The photovoltaic (PV) sector has a fundamental role to cover the energy demand. To date, the PV market is based mainly on the "first generation" technology, i.e., monocrystalline and polycrystalline silicon, because of high conversion efficiency of solar radiation into electricity. Despite that, the expensive manufacturing processes of silicon and its decreasing availability in nature have accelerated the "second generation" thin-film technologies exploitation based on materials such as cadmium telluride (CdTe) and amorphous silicon (a-Si) [2]. Besides this, The "third generation" PV aims to keep high efficiency by reducing production costs thanks to hybrid-organic materials on rigid and flexible substrates [3–6]. Natural dyes such as anthocyanins [7], polymers [8] or fullerenes [9] are just a few examples of molecules used for this purpose. The main issue concerning these new technologies is the stability, since the organic molecules used are very sensitive to the operating conditions, such as temperature, prolonged exposure to UV light, humidity. The materials toxicity of the materials used and the synthesis/purification costs are issues to be addressed.

In the recent years, Perovskite (PVSK) is widely used as photo-generator [10–12]. Its optical and electronic properties allowed a continuous development reaching record efficiencies (close to 26%) in a few years [13]. PVSK is a chemical compound with ABX_3 formula, where A and B are cations with different atomic radii and X represents an anion. Currently by PVSKs, we refer to all crystalline solids with the same structure as $CaTiO_3$ (bipyramidal crystalline cell with square base). Recently perovskite-based materials organometallic compounds of halogens have gathered particular interest in PV field thanks to the easy processability by solution together with efficiency comparable to the best inorganic materials used in optoelectronics such as gallium arsenide (GaAs) and Si.

Typically, a PVSK solar cell (PSC) is a layered structure, where each layer performs a well-defined function affecting the performance and the stability of the device. The PVSK is sandwiched between one electron transport layer (ETL) and a hole transport layer (HTL). ETL and HTL are both connected to an external circuit by gold or silver contacts. In case of n-i-p architecture, ETL is generally composed by c-TiO_2 (compact TiO_2) and mp-TiO_2 (mesoporous TiO_2) or SnO_2 and guarantee good conduction, low charge recombination and high transparency. The most widespread HTL is the 2,2′,7,7′-Tetrakis(N,Ndi-p-methoxyphenylamine)-9,9′- spirobifluorene. Spiro-MeOTAD ensures good energy levels of band gap, quick charge transfer and low recombination, however there are still many related problems to the use of this material, e.g., operational environment sensitivity, high cost (about 200 euro/g), complex synthesis and low yield [14]. Moreover, spiro-OMeTAD is doped to increase the mobility of the holes with highly hygroscopic salts (lithiumbis(trifluoromethylsulfonyl)imide (Li-TFSI) or 4-tert-butylpyridine (t-BP)) leading to PSC degradation deterioration. About the metal counter-electrode, gold diffuses into the structure of the device when exposed to continuous lighting, damaging it. It is possible to replace both the organic HTL and the metal electrode with one low temperature conductive carbon layer. Carbon materials are cheap if compared to HTMs (hole transporting materials) and gold, resulting in a reduction of cells cost and an increase in stability. Carbon is a key material widely used in the PV field due to its abundance, low cost, and appropriate energy level. Different kind of carbon materials [15–17], such as carbon nanotubes, carbon fiber, graphene have been applied with success in many PV devices. In the PVSK field, the efficiencies are competitive with those measured in devices using spiro-OMeTAD as HTM [18–23]. Low temperature carbon pastes, unlike the porous high temperature inks [17,21], can be processed at temperatures below 130 °C exhibiting features of high conductivity, low cost, good stability and high throughput process.

In this paper, we demonstrate a simple process to fabricate HTL- and gold-free PSCs based on low temperature carbon counter-electrode by adopting solution-based processes for the full cell stack.

2. Materials and Methods

We adopted large area (1.01 cm^2) n-i-p cells as reported in Figure 1a.

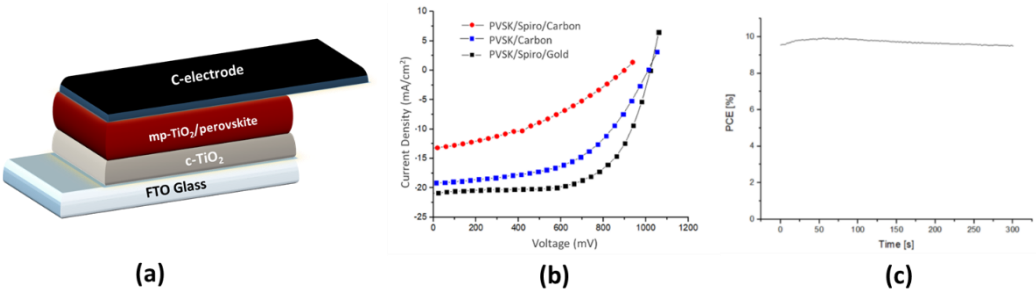

Figure 1. (**a**) PSC layers; (**b**) JV curves measurements; (**c**) Stability by MPP tracking.

We cleaned the FTO (fluorinated tin oxide) glasses (NSG, 8 Ω/sq.) in an ultrasonic system by using subsequent solvents (soap/water, acetone, ethanol and isopropanol) for 5 min each. We deposited 30 nm thick c-TiO_2 as reported in [24] and 250 nm thick mp-TiO_2 paste (Great Cell Solar 18 nrt, diluted with ethanol 1:4 *w*/*w*) is by spin coating method followed by 30 min@500 °C sintering in oven. The substrates are exposed to an UV lamp and then we deposited the triple cation PVSK ($Cs_{0.05}(MA_{0.17}FA_{0.83})_{0.95}Pb(I_{0.83}Br_{0.17})_3$ in DMF/DMSO, 1.42 M) (PbI_2 from TCI Co., Ltd.; CsI, FAI and MABr from Great Cell Solar) by spin-coating method in a glove-box. The spin-coating parameters to deposit the precursor solution are as follow: 1st step at 1000 rpm, 5 s ramping, 10 s; 2nd step 5000 rpm, 2s ramping, 30 s; chlorobenzene dropped 7 s before the end. Then, the PVSK is annealed 60 min@100 °C. In a recent publication we demonstrated how to scale-up the triple cation

PVSK formulation to module device [24]. About the gold-based cells, Spiro-OMeTAD (Borum) HTM solution is prepared and deposited according to [14]. Following this, 85 nm-thick gold and 30 μm carbon (Dyenamo) counter-electrodes are thermally evaporated and blade-coated, respectively. The carbon-based cells are annealed at 60 °C in vacuum and 120 °C in air for 15 min in case of Spiro HTM and HTM-free, respectively. The JV curves and the stability measurements are reported by a Keithley source meter/LabVIEW under a class A sun simulator (Sun 2000, Abet) at AM 1.5 1000 W/m^2 calibrated by a Skye Instruments sensor Ltd.

3. Results and Discussion

The JV curves are depicted in Figure 1b and Table 1.

Table 1. Electrical parameters of the fabricated devices. HI is the Hysteresis Index [25].

Cell Stack	Voc (V)	Jsc (mA/cm^2)	FF (%)	PCE (%)	HI
TiO_2/PVSK/Spiro/Carbon	0.90	12.67	39	4.40	1.20
TiO_2/PVSK/Carbon	1.01	19	53	10.20	1.05
TiO_2/PVSK/Spiro/Gold	1.02	20.30	65	13.40	1.25

In case of PVSK/Spiro/carbon cells all the electrical parameters are lower with respect to the PVSK/carbon cells. Most likely capacitive and recombination phenomena occur at Spiro/Carbon interface this inefficient set up affecting not only the fill factor, but also current and Voc. A lower FF mainly affects the PCE by comparing PVSK/carbon with PVSK/HTL/Gold cells, because of less conductivity of carbon electrode with respect to the gold one. It is also important to underline how the hysteresis phenomena are practically absent in the case of carbon-based cells by comparing the hysteresis index (HI) in Table 1 [26]. In case of PVSK/carbon cells, the short circuit current density (J_{sc}) is about 19 mA/cm^2, as reported in Figure 1b and Table 1. The best efficiencies are 13.4% and 10.2% for the PVSK/HTL/Gold and PVSK/Carbon devices, respectively (Figure 1b, Table 1). After 5 min in light condition at maximum power point the device loses just 4% efficiency and keeps stable at 9.8% (Figure 1c, Table 1).

4. Conclusions

The PV exploitation should avoid high-cost and high-CO_2 footprint materials and fabrication processes. The adoption of low-temperature carbon PSC counter-electrodes permits to avoid expensive organic HTM and metal counter-electrodes, such as gold or silver. These materials are also source of degradation leading to low stability in presence of moisture, temperature and light. Moreover, the carbon inks can be deposited by large area printing techniques, such as screen-printing and blade-coating. Since the carbon layer can be annealed at temperature less than 120 °C, the impact from the LCA (life cycle assessment) point of view is low. Here, we demonstrated how the PSCs can work without any HTL losing low efficiency. Further studies on low cost 2D PVSK strategies are in the pipeline to improve the electrical parameters of the cells. Moreover, the scaling up to module and stability assessment according to ISOS standard is ongoing.

Author Contributions: Conceptualization, L.V.; methodology, L.V.; validation, L.V. and A.D.C.; formal analysis, L.V. and M.S.; investigation, M.S. and L.V.; resources, A.D.C.; data curation, L.V. and M.S.; writing—original draft preparation, L.V.; writing—review and editing, L.V.; visualization, L.V.; supervision, A.D.C. and L.V.; project administration, A.D.C. and L.V.; funding acquisition, A.D.C. and L.V. All authors have read and agreed to the published version of the manuscript.

Funding: This research was funded by the European Union's Horizon 2020 programme, through an FET Proactive research and innovation action under grant agreement No. 101084124 (DIAMOND). The authors acknowledge the project UNIQUE, supported under the umbrella of SOLARERA.NET_cofund by ANR, PtJ, MUR (GA 775970), MINECOAEI, SWEA, within the European Union

Framework Program for Research and Innovation Horizon 2020 (Cofund ERANET Action, No. 691664).

Data Availability Statement: Data supporting reported results are available in repository.

Conflicts of Interest: The authors declare no conflict of interest.

References

1. Eftekharnejad, S.; Vittal, V.; Heydt, G.T.; Keel, B.; Loehr, J. Impact of increased penetration of photovoltaic generation on power systems. *IEEE Trans. Power Syst.* **2013**, *28*, 893–901. https://doi.org/10.1109/TPWRS.2012.2216294.
2. Barkhouse, D.A.R.; Gunawan, O.; Gokmen, T.; Todorov, T.K.; Mitzi, D.B. Yield predictions for photovoltaic power plants:empirical validation,recent advances and remaining uncertainties. *Prog. Photovolt. Res. Appl.* **2015**, *20*, 6–11. https://doi.org/10.1002/pip.
3. Mincuzzi, G.; Vesce, L.; Liberatore, M.; Reale, A.; Di Carlo, A.; Brown, T.M. Laser-sintered TiO_2 films for dye solar cell fabrication: An electrical, morphological, and electron lifetime investigation. *IEEE Trans. Electron Devices* **2011**, *58*, 3179–3188. https://doi.org/10.1109/TED.2011.2160643.
4. Barichello, J.; Vesce, L.; Mariani, P.; Leonardi, E.; Braglia, R.; Di Carlo, A.; Canini, A.; Reale, A. Stable semi-transparent dye-sensitized solar modules and panels for greenhouse application. *Energies* **2021**, *14*, 6393. https://doi.org/10.3390/en14196393.
5. Zardetto, V.; De Angelis, G.; Vesce, L.; Caratto, V.; Mazzuca, C.; Gasiorowski, J.; Reale, A.; Di Carlo, A.; Brown, T.M. Formulations and processing of nanocrystalline TiO_2 films for the different requirements of plastic, metal and glass dye solar cell applications. *Nanotechnology* **2013**, *24*, 255401. https://doi.org/10.1088/0957-4484/24/25/255401.
6. Dominici, L.; Vesce, L.; Colonna, D.; Michelotti, F.; Brown, T.M.; Reale, A.; Di Carlo, A. Angular and prism coupling refractive enhancement in dye solar cells. *Appl. Phys. Lett.* **2010**, *96*, 42. https://doi.org/10.1063/1.3328097.
7. Yuvapragasam, A.; Muthukumarasamy, N.; Agilan, S.; Velauthapillai, D.; Senthil, T.S.; Sundaram, S. Natural dye sensitized TiO_2 nanorods assembly of broccoli shape based solar cells. *J. Photochem. Photobiol. B Biol.* **2015**, *148*, 223–231. https://doi.org/10.1016/j.jphotobiol.2015.04.017.
8. Etxebarria, I.; Ajuria, J.; Pacios, R. Solution-processable polymeric solar cells: A review on materials, strategies and cell architectures to overcome 10%. *Org. Electron.* **2015**, *19*, 34–60. https://doi.org/10.1016/j.orgel.2015.01.014.
9. Zhang, G.; Ning, H.; Chen, H.; Jiang, Q.; Jiang, J.; Han, P.; Dang, L.; Xu, M.; Shao, M.; He, F.; et al. Naphthalenothiophene imide-based polymer exhibiting over 17% efficiency. *Joule* **2021**, *5*, 931–944. https://doi.org/10.1016/j.joule.2021.02.003.
10. Kojima, A.; Teshima, K.; Shirai, Y.; Miyasaka, T. Organometal halide perovskites as visible-light sensitizers for photovoltaic cells. *J. Am. Chem. Soc.* **2009**, *131*, 6050–6051. https://doi.org/10.1021/ja809598r.
11. Snaith, H.J. Present status and future prospects of perovskite photovoltaics. *Nat. Mater.* **2018**, *17*, 372–376. https://doi.org/10.1038/s41563-018-0071-z.
12. Feng, S.-P.; Cheng, Y.; Yip, H.-L.; Zhong, Y.; Fong, P.W.K.; Li, G.; Ng, A.; Chen, C.; Castriotta, L.A.; Matteocci, F.; et al. Roadmap on Commercialization of Metal Halide Perovskite Photovoltaics. *J. Phys. Mater.* **2023**. https://doi.org/10.1088/2515-7639/acc893.
13. Green, M.A.; Dunlop, E.D.; Hohl-Ebinger, J.; Yoshita, M.; Kopidakis, N.; Bothe, K.; Hinken, D.; Rauer, M.; Hao, X. Solar cell efficiency tables (Version 60). *Prog. Photovolt. Res. Appl.* **2022**, *30*, 687–701. https://doi.org/10.1002/pip.3595.
14. Vesce, L.; Stefanelli, M.; Di Carlo, A. Efficient and stable perovskite large area cells by low-cost fluorene-xantene-based hole transporting layer. *Energies* **2021**, *14*, 6081. https://doi.org/10.3390/en14196081.
15. Calabrò, E.; Matteocci, F.; Paci, B.; Cinà, L.; Vesce, L.; Barichello, J.; Generosi, A.; Reale, A.; Di Carlo, A. Easy Strategy to Enhance Thermal Stability of Planar PSCs by Perovskite Defect Passivation and Low-Temperature Carbon-Based Electrode. *ACS Appl. Mater. Interfaces* **2020**, *12*, 32536–32547. https://doi.org/10.1021/acsami.0c05878.
16. Barichello, J.; Vesce, L.; Matteocci, F.; Lamanna, E.; Di Carlo, A. The effect of water in Carbon-Perovskite Solar Cells with optimized alumina spacer. *Sol. Energy Mater. Sol. Cells* **2019**, *197*, 76–83. https://doi.org/10.1016/j.solmat.2019.03.029.
17. Vesce, L.; Riccitelli, R.; Mincuzzi, G.; Orabona, A.; Soscia, G.; Brown, T.M.; Di Carlo, A.; Reale, A. Fabrication of spacer and catalytic layers in monolithic dye-sensitized solar cells. *IEEE J. Photovolt.* **2013**, *3*, 1004–1011. https://doi.org/10.1109/JPHOTOV.2013.2262374.
18. Stefanelli, M.; Vesce, L.; Di Carlo, A. Upscaling of Carbon-Based Perovskite Solar Module. *Nanomaterials* **2023**, *13*, 313. https://doi.org/10.3390/nano13020313.
19. Liu, Z.; Shi, T.; Tang, Z.; Sun, B.; Liao, G. Using a low-temperature carbon electrode for preparing hole-conductor-free perovskite heterojunction solar cells under high relative humidity. *Nanoscale* **2016**, *8*, 7017–7023. https://doi.org/10.1039/c5nr07091k.
20. Chu, Q.Q.; Ding, B.; Qiu, Q.; Liu, Y.; Li, C.X.; Li, C.J.; Yang, G.J.; Fang, B. Cost effective perovskite solar cells with a high efficiency and open-circuit voltage based on a perovskite-friendly carbon electrode. *J. Mater. Chem. A* **2018**, *6*, 8271–8279. https://doi.org/10.1039/c7ta10871k.
21. Bogachuk, D.; Zouhair, S.; Wojciechowski, K.; Yang, B.; Babu, V.; Wagner, L.; Xu, B.; Lim, J.; Mastroianni, S.; Pettersson, H.; et al. Low-Temperature Carbon-based Electrodes in Perovskite Solar Cells. *Energy Environ. Sci.* **2020**, *13*, 3880–3916. https://doi.org/10.1039/D0EE02175J.

22. Jiang, P.; Jones, T.W.; Duffy, N.W.; Anderson, K.F.; Bennett, R.; Grigore, M.; Marvig, P.; Xiong, Y.; Liu, T.; Sheng, Y.; et al. Fully printable perovskite solar cells with highly-conductive, low-temperature, perovskite-compatible carbon electrode. *Carbon* **2018**, *129*, 830–836.
23. Lin, S.; Yang, B.; Qiu, X.; Yan, J.; Shi, J.; Yuan, Y.; Tan, W.; Liu, X.; Huang, H.; Gao, Y.; et al. Efficient and stable planar hole-transport-material-free perovskite solar cells using low temperature processed SnO_2 as electron transport material. *Org. Electron.* **2018**, *53*, 235–241. https://doi.org/10.1016/j.orgel.2017.12.002.
24. Vesce, L.; Stefanelli, M.; Herterich, J.P.; Castriotta, L.A.; Kohlstädt, M.; Würfel, U.; Di Carlo, A. Ambient Air Blade-Coating Fabrication of Stable Triple-Cation Perovskite Solar Modules by Green Solvent Quenching. *Sol. RRL* **2021**, *5*, 2100073. https://doi.org/10.1002/solr.202100073.
25. Chen, B.; Yang, M.; Priya, S.; Zhu, K. Origin of J-V Hysteresis in Perovskite Solar Cells. *J. Phys. Chem. Lett.* **2016**, *7*, 905–917. https://doi.org/10.1021/acs.jpclett.6b00215.
26. Ren, J.; Kan, Z. *Chapter 1: Origin of Hysteresis in Perovskite Solar Cells*; AIP Publishing LLC: Melville, NY, USA, 2020; Volume 1, ISBN 9780735422414.
27. Vesce, L.; Guidobaldi, A.; Mariani, P.; Di Carlo, A.; Parisi, M.L.; Maranghi, S.; Basosi, R. Scaling-up of Dye Sensitized Solar Modules. In *World Scientific Reference of Hybrid Materials*; World Scientific: Singapore, 2019; Volume 2, pp. 423–485.